metals

MDPI

Article

TIG Dressing Effects on Weld Pores and Pore Cracking of Titanium Weldments

Hui-Jun Yi [1,*], Yong-Jun Lee [2] and Kwang-O Lee [3]

[1] Hyundai-Rotem Company, Chang-won 51407, Korea
[2] The 3rd land system team, Defense Agency for Technology and Quality, Chang-won 51472, Korea; elan4017@naver.com
[3] School of Mechanical Engineering, Pusan National University, Busan 46287, Korea; royallko@pusan.ac.kr
* Correspondence: yi.h.jun@gmail.com; Tel.: +82-10-4846-3184

Academic Editor: Giuseppe Casalino
Received: 10 August 2016; Accepted: 10 October 2016; Published: 17 October 2016

Abstract: Weld pores redistribution, the effectiveness of using tungsten inert gas (TIG) dressing to remove weld pores, and changes in the mechanical properties due to the TIG dressing of Ti-3Al-2.5V weldments were studied. Moreover, weld cracks due to pores were investigated. The results show that weld pores less than 300 μm in size are redistributed or removed via remelting due to TIG dressing. Regardless of the temperature condition, TIG dressing welding showed ductility, and there was a loss of 7% tensile strength of the weldments. Additionally, it was considered that porosity redistribution by TIG dressing was due to fluid flow during the remelting of the weld pool. Weld cracks in titanium weldment create branch cracks around pores that propagate via the intragranular fracture, and oxygen is dispersed around the pores. It is suggested that the pore locations around the LBZ (local brittle zone) and stress concentration due to the pores have significant effects on crack initiation and propagation.

Keywords: titanium welding; weld pores; cracks; TIG dressing; ductility

1. Introduction

High strength, low density, and excellent corrosion resistance are the main properties of titanium that make it attractive for a variety of applications. A variety of welding methods have been used for titanium alloys, and several studies of high-energy welding using lasers and new welding methods, such as friction stir welding, have been conducted. The welding method most widely used in industrial applications is the tungsten inert gas (TIG) welding process. The main advantages of TIG, in comparison with other welding methods, are its cost-effectiveness, workability, and ease of use. When a titanium alloy is welded using a fusion welding method such as TIG, the titanium alloy bonds easily with oxygen, nitrogen, and carbon at temperatures over 500 °C, which results in a high degree of brittleness. Therefore, the weldment needs to be protected or shielded from ambient air. The primary precaution taken is shielding the metal from any contact with air, hydrogen, carbon compounds, or other contaminants during the melting, solidification, and solid-state cooling processes associated with fusion welding. To prevent contamination, the weld joint and weld electrode must be clean, and the shielding gas (usually argon, but sometimes helium or a mixture of the two) must be free of moisture and other impurities. The torch used in the TIG process is designed to permit an inert gas to flow through it, surrounding the electrode and molten metal pool with a protective atmosphere. In addition, a trailing shield of inert gas should be used to protect the weldment while it is solidifying.

Apart from the problem of oxidation at high temperatures, the most frequently occurring problem in the welding of titanium alloys is porosity and its effects, which are the main subjects of this study [1–3]. Weld metal porosity in a titanium alloy is known to originate at the trailing edge of the

weld pool, where interstitial elements (oxygen or hydrogen) are partitioned between dendrites during solidification. Partitioning occurs because of the large decrease in oxygen (or hydrogen) solubility that occurs in the transformation from liquid to solid. There are several gaseous species that could become trapped during the welding of titanium. The most likely of these is hydrogen, but other possible agents include oxygen, nitrogen, and carbon dioxide, as well as the inert shielding gases. These gases could be present as a result of any of the following: (a) desorption of the gases' elemental constituents from the parent material or welding consumables; (b) absorption into the weld pool due to inadequate shielding (through either entrapment of air in the shielding gases or a high moisture level in the shielding gases) during welding; (c) entrapment of the shielding gases; or (d) surface contamination [4–9].

Various methods, including variation of the process parameters and attention to cleanliness, have been employed to attempt to minimize porosity in titanium weldments. Removal of the hydrated layers prior to welding is critical to minimizing the potential hydrogen content of the melt pool. Consequently, the effectiveness of the method used to remove the hydrated layer and other surface contaminants may have a large influence on the weld metal porosity. In addition to the above methods for ensuring cleanliness of the titanium material prior to welding, relatively low heat input conditions and a high welding speed have been recommended to reduce the porosity of weldments for TIG and EBW (electron beam welding) [10–13]. Additionally, a new welding process was studied [14].

The effects of dispersed pores in weldments vary. Although an allowable level of porosity is specified in welding structure designs, depending on the importance of the structure, the aviation and power generation facility sectors, in which titanium alloys are widely used, regulate porosity in weldments strictly. Although the effects of porosity in weldments vary, porosity in titanium weldments is reported to result in pore cracking that initiates at the pores in the weldments. Pore cracking in titanium welds is known to occur mainly in restrained sections. Recent studies have found that alloys with hydrogen contents greater than 200 wt ppm are more prone to pore cracking and that the probability of cracking increases with increased porosity. Previous studies have attempted to explain pore cracking in Ti-6211 welds in terms of oxygen embrittlement. Therefore, the current thinking tends to associate pore cracking in titanium welds with interstitial (oxygen, hydrogen, and so forth) embrittlement [15–19].

The soundness of weldments and the presence of pores can be verified using nondestructive test methods, such as X-ray testing, after titanium alloy welding. If pores are detected in weldments, the portion of the weld in which the pores are present can be removed mechanically. This is followed by repair welding, i.e., re-welding, as required. However, this process is known to degrade the mechanical strength of weldments. In addition, complex processes, such as the complete removal of surface oxides using the chemical pickling method, must be performed prior to welding to remove the cause of the formation of pores completely. This not only reduces weld joint efficiency but also has a number of adverse effects on productivity. In this study, TIG dressing was used to remove welding pores generated in weldments more simply and effectively than has been accomplished previously using other methods. Pores in Ti-3Al-2.5V titanium alloy weldments used in power generation facilities were examined in this study, and the causes of the pore cracking phenomenon that occurs as a result of the presence of pores were analyzed. In addition, the effects of the redistribution and removal of pores formed in Ti-3Al-2.5V titanium alloy weldments via TIG dressing and the effects of TIG dressing on the strength and toughness of titanium alloy weldments at a high temperature condition were examined.

2. Materials and Methods

2.1. The Effect of TIG Dressing

To examine the effectiveness of TIG dressing in removing weld porosity in titanium alloy weldments and the effects of TIG dressing on the mechanical properties of the weldments, a specimen was manufactured using a 2.0-mm-thick Ti-3Al-2.5V alloy, as shown in Figure 1. Normally, the objective of TIG dressing is to remove welding geometrical imperfections, such as undercut by remelting the

weld toe, thereby leaving the weld practically free of geometric defects. The treatment also significantly reduces the stress concentration factor of the weld toe by introducing a smooth transition. Therefore, the TIG dressing is used to improve the fatigue life of welded structures [20–22]. In this study, standard TIG welding equipment was used, without the addition of any filler material. The chemical composition of the base metal and filler metal are given in Table 1. The TIG welding was performed with 99.9% argon gas used as the shielding and purging gas. A fully equipped out-of-chamber purging device and an automatic welding machine were used to protect against oxidation during welding as shown in Figure 2. Table 2 gives the parameters of the welding and TIG dressing.

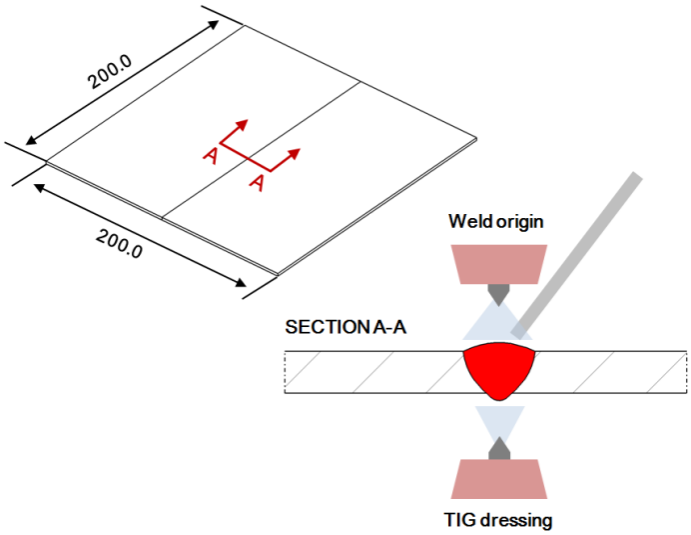

Figure 1. Illustration of welding test of Ti-3Al-2.5V and tungsten inert gas (TIG) dressing.

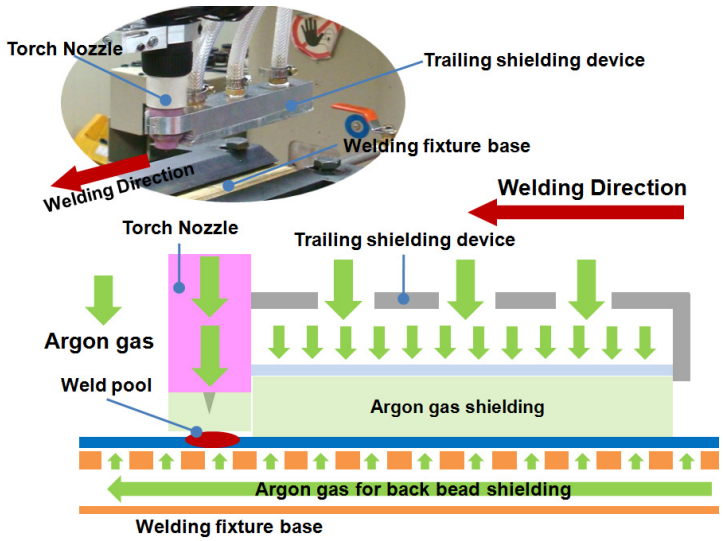

Figure 2. Illustration of out-of-chamber welding test equipment.

Table 1. Chemical compositions of base metal and filler metal (wt %).

Identification	C	Fe	Al	V	N	O	H	Ti
Base metal	0.03	0.25	3.02	2.49	0.02	0.12	0.005	Bal.
Filler metal	0.02	0.01	2.98	2.48	0.01	0.10	0.001	Bal.

Table 2. Welding and TIG dressing parameters.

Identification		Ampere (A)	Voltage (V)	Welding Speed (cm/min)	Welding Feeding Speed (cm/min)	Remark
Specimen A	WO	58	9.2	25	34	Original weldment
	R01	68	9.8	25	-	1st TIG dressing
Specimen B	WO	58	9.2	25	34	Original weldment
	R01	68	9.8	25	-	1st TIG dressing
	R02	68	9.8	25	-	2nd TIG dressing
Specimen C	WO	58	9.2	25	34	Original weldment
	R01	68	9.8	25	-	1st TIG dressing
	R02	68	9.8	25	-	2nd TIG dressing
	R03	68	9.8	25	-	3rd TIG dressing

To assess the effectiveness of the TIG dressing, a specimen was manufactured from which oxide films of the titanium alloy were not removed. After 48 h had elapsed since welding, X-ray testing was done to verify the presence of pores in the weldment and to determine pore distribution. After the first X-ray test on the specimen, the TIG dressing was conducted at a location at which a back bead in the weldment had formed, as shown in Figure 1. After the first TIG dressing was completed, X-ray testing was conducted at three times. At the time of the TIG dressing welding, the oxide film on the titanium alloy surface was not removed using a mechanical or chemical method. After the original welding and TIG dressing, X-ray inspection was performed to check for the existence of pores and to determine the pore distribution. For the X-ray test equipment, both the X-ray generator and tube used MG452 YXLON (YXLON, Hudson, NY, USA) to ensure that the required resolution was obtained. The scale bar on the radiographic film was used to confirm the pore sizes.

To assess the changes in the mechanical properties of the weldment due to the TIG dressing, tensile tests and notched tensile tests were conducted. Tensile and notch tensile specimens were prepared as per the ASTM E8M-05 standard test method as shown in Figure 3. The tensile tests were carried out in a 100 kN universal testing machine (Instron 8501, INSTRON, Norwood, MA, USA). The specimens were loaded at a rate of 1.5 kN/min, as per the ASTM standard. The tensile tests were performed at 25 °C, 300 °C, and 500 °C. At each conditions, three tensile and notch tensile specimens were used.

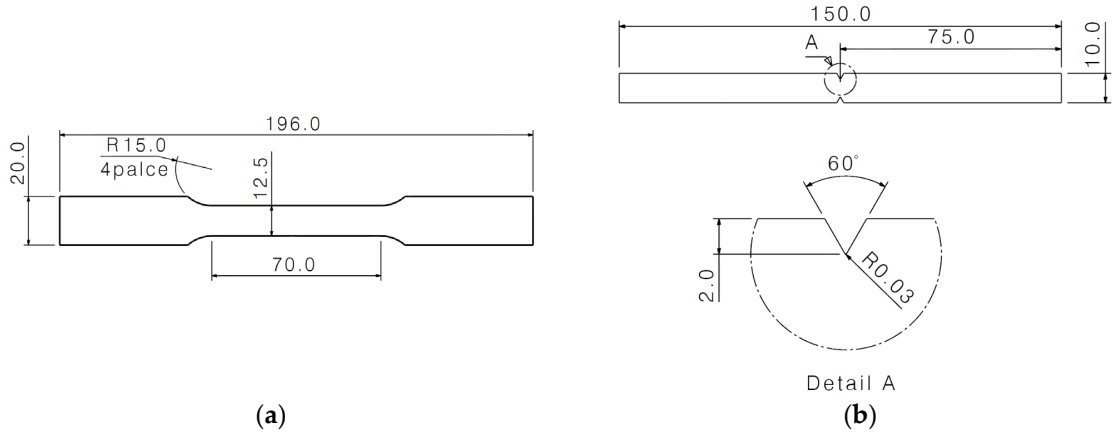

Figure 3. Illustration of tensile and notched tensile specimen: (**a**) tensile test; (**b**) notch tensile test.

2.2. Pore Craking Problems

Figure 4 shows cracks occurred Ti-3Al-2.5V (2.0-mm-thick) pipes used to move sea water in a power generation facility. Cracks also occurred in the weldments of brackets used to assemble the

pipes. The cracks were observed approximately one week after the welding. The mechanical properties and chemical composition of the material used are shown in Table 1. The welding was done with the TIG welding and welding parameters are summarized in Table 3. The oxide film on the surfaces of the weldments was removed using a stainless steel brush prior to welding.

To observe the cracks in the weldments, cracked parts were removed from the structure, and the fractured cross section and microstructure of each weldment were examined using optical microscopy (OLYMPUS, Tokyo, Japan) and scanning electron microscopy (SEM, SERON, Uiwang-si, Korea). To determine the probable cause of the cracks, cross sections of cracked specimens were first observed with an optical microscope and then intentionally fractured using a tensile and bending test apparatus (Instron 8501, INSTRON, Norwood, MA, USA). The fracture surfaces were investigated with SEM to determine the fracture mode.

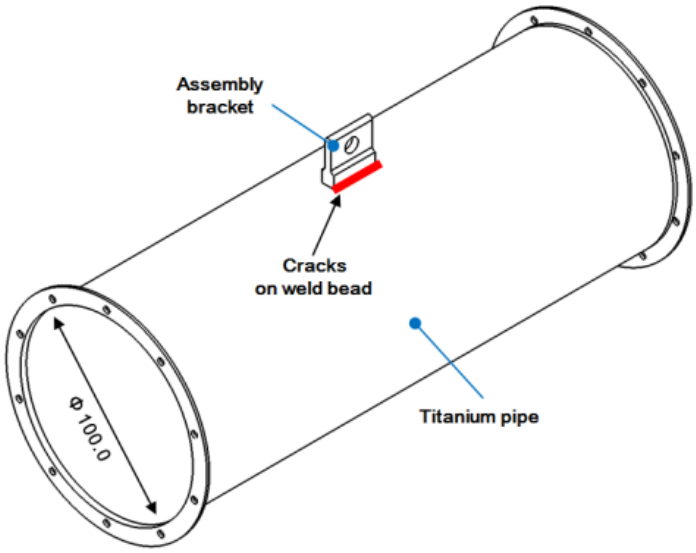

Figure 4. Illustration of cracks occurred Ti-3Al-2.5V pipe weldment.

Table 3. Welding parameters of Ti-3Al-2.5V pipe.

Ampere (A)	Voltage (V)	Welding Speed (cm/min)	Remark
75.0	10.5	25	

3. Results

3.1. Weld Porosity Redistribution Due to the TIG Dressing

Table 4 and Figure 5 show the X-ray test results and weld porosity redistribution results. The weld pore sizes were mostly within the range of 100 to 250 μm, with a few pores exceeding 250 μm in size. When the TIG dressing was conducted on the first WO weldment, the number of weld pores decreased. The change in the number of pores was detected after the first TIG dressing; the second and third TIG dressings produced no change in the number of pores or in the pore sizes. Furthermore, pores greater than 300 μm in size were not removed, nor were their sizes redistributed or reduced, by the remelting that resulted from the TIG dressing. Figure 6 shows the SEM images of the pore distribution of the WO. Large-scale SEM microscopy indicated that the inner surfaces of the pores were smooth, as shown in Figure 7. The round shapes and smooth inner surfaces suggest that the pores were formed as a result of gas evolution during the welding.

Table 4. Results of X-ray inspection, quantity, and size of pores (d).

Identification		$d \leq 150$ μm	150 μm< $d \leq 250$ μm	250 μm< $d \leq 500$ μm
Specimen A	WO	10	19	2
	R01	3	8	2
Specimen B	WO	12	28	2
	R01	3	12	2
	R02	3	12	2
Specimen C	WO	2	10	5
	R01	1	4	5
	R02	1	4	5
	R03	1	4	5

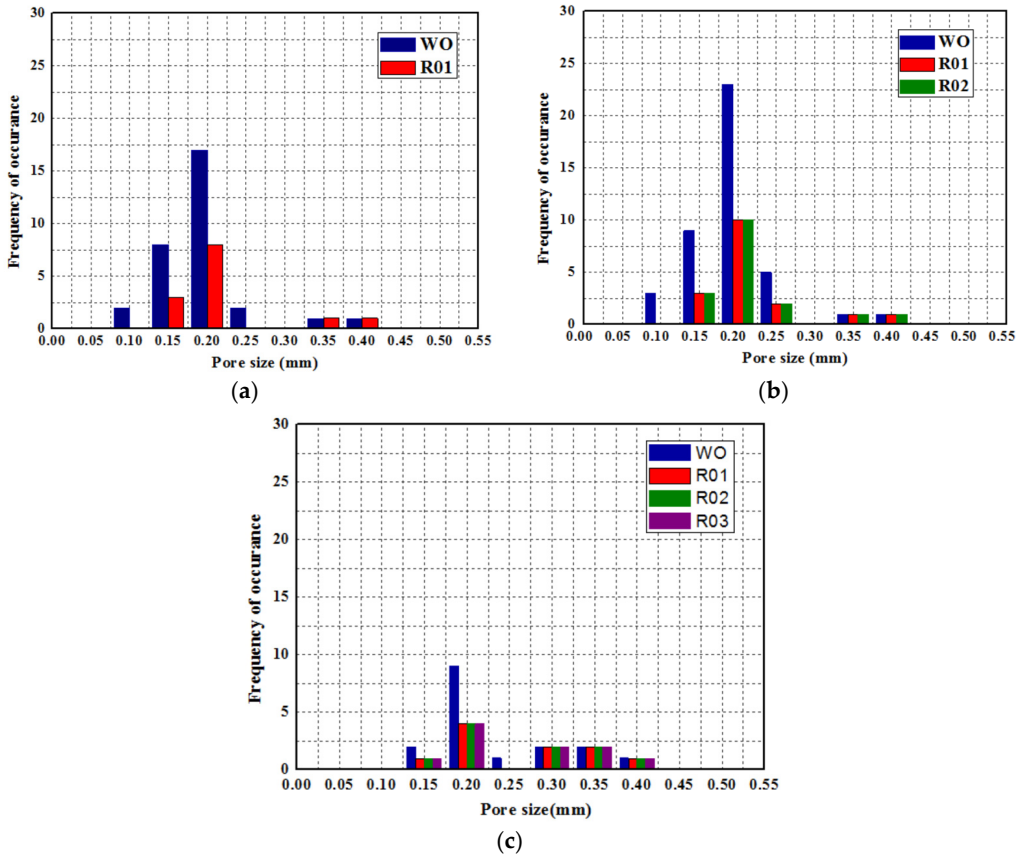

Figure 5. Effect of TIG dressing on porosity removing and distribution: (a) specimen A; (**b**) specimen B; (**c**) specimen C.

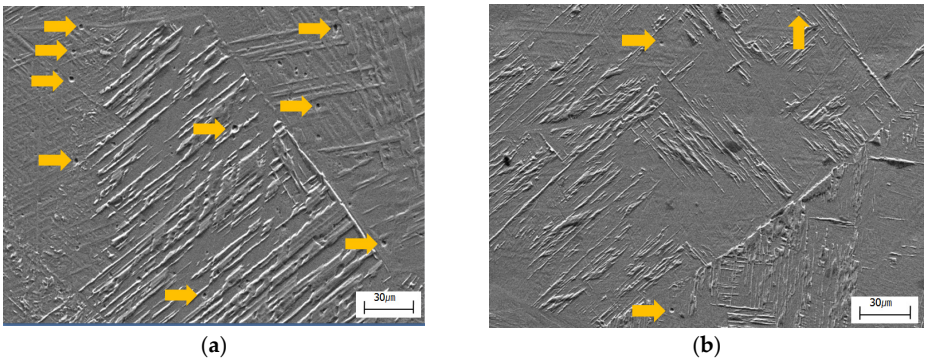

Figure 6. SEM image of pores in weld metal: Yellow arrows indicate pores: (**a**) WO; (**b**) R03.

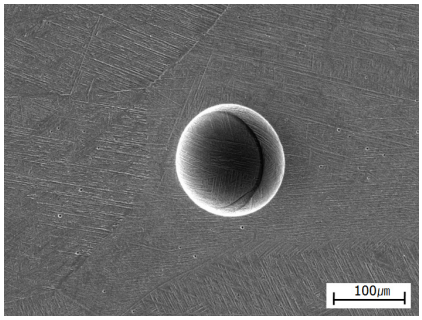

Figure 7. SEM image of pores (≥100 μm) in weld metal (WO).

3.2. *Effect of the TIG Dressing on Mechanical Properties of the Weldment*

The tensile test results for the WO and TIG dressings for ambient- and high-temperature conditions are shown in Figure 8. At every temperature, the ultimate tensile strength was decreased in comparison to the pretreatment strength, but not much change was observed between the first treatment and the second and third treatments. The notch toughness properties (NSR, notch strength ratio = notch tension strength/tension strength) for ambient- and high-temperature conditions are shown in Figure 9. Regardless of the temperature condition and the number of TIG dressing applications, all of the weldments have ductile properties.

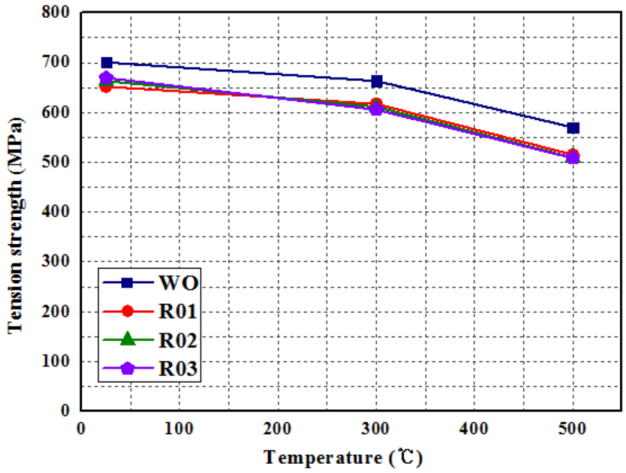

Figure 8. Results of the tensile strength test.

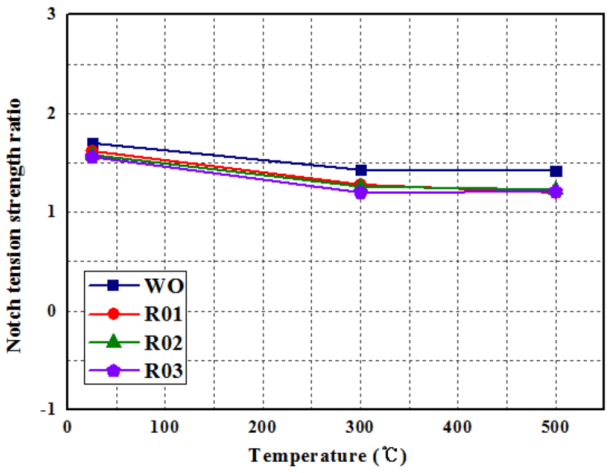

Figure 9. Results of the NSR (notch tension strength ratio).

3.3. Observation of the Microstructure of the Cracked Specimen

Metallographic examinations were conducted on the cracked specimens. Figure 10 shows the microstructure of the weldment and the heat-affected part, in which an acicular α, α′, and a prior β grain boundary generated in the Ti-3Al-2.5V weldment were observed. The SEM results showed that weldment porosity was distributed over areas where cracks were formed, as shown in Figure 11. After the metallographic examinations were completed, the cracked specimens were opened and examined via SEM as shown in Figure 12. Observation of the cracks' fracture shapes revealed that cracking progressed as intragranular fracture and that small branch cracks were created during the crack propagation. That is, the propagation of the cracks formed in the Ti-3Al-2.5V alloy weldment progressed along the columnar grain boundaries through the intragranular fracture and that small branch cracks were formed as the propagation progressed.

To identify the causes of the pore formation, the chemical composition of the weld material around the pores was determined using energy dispersive spectroscopy (EDS). The results are shown in Table 5 and Figure 13. The EDS results show that the pores and the surrounding areas had higher oxygen contents than other areas, which confirms that the main cause of the porosity was oxidation. The oxide films formed in the titanium alloy surface during welding reacted with carbon in the atmosphere to form CO and CO_2, which are known to be the main cause of pore formation.

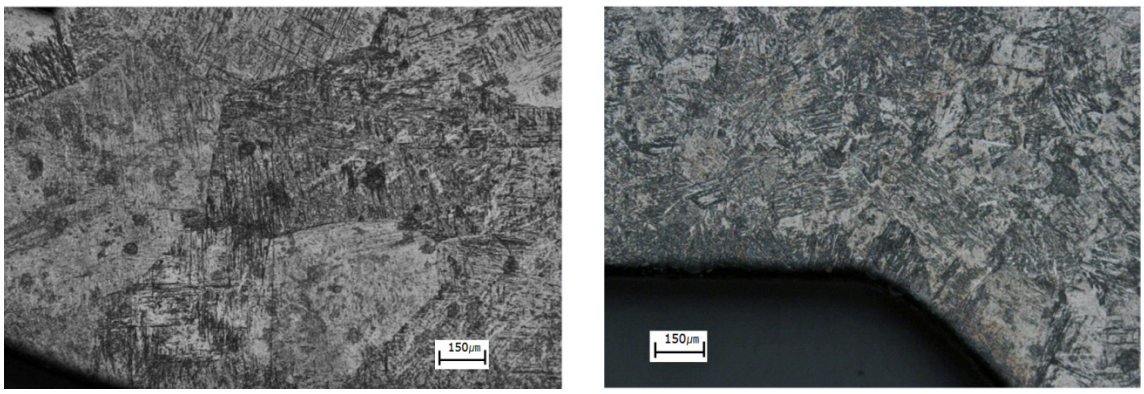

(**a**) (**b**)

Figure 10. Optical image of Ti-3Al-2.5V pipe weldment: (**a**) weld metal; (**b**) heat affected zone.

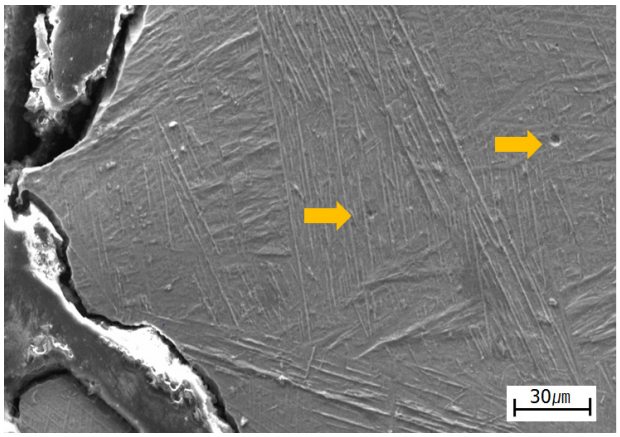

Figure 11. SEM image of cracked Ti-3Al-2.5V pipe weldment: yellow arrows indicate pores.

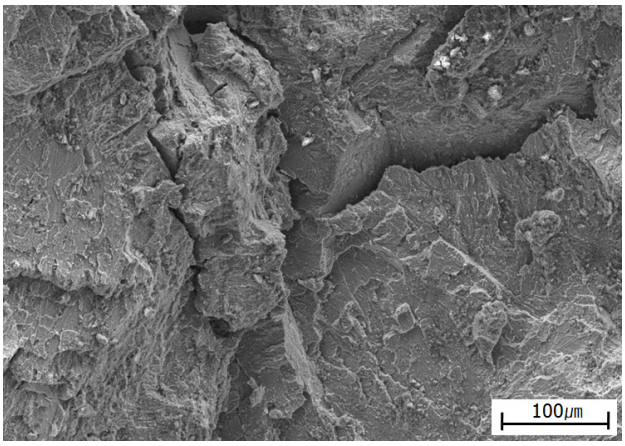

Figure 12. SEM image of fracture surface.

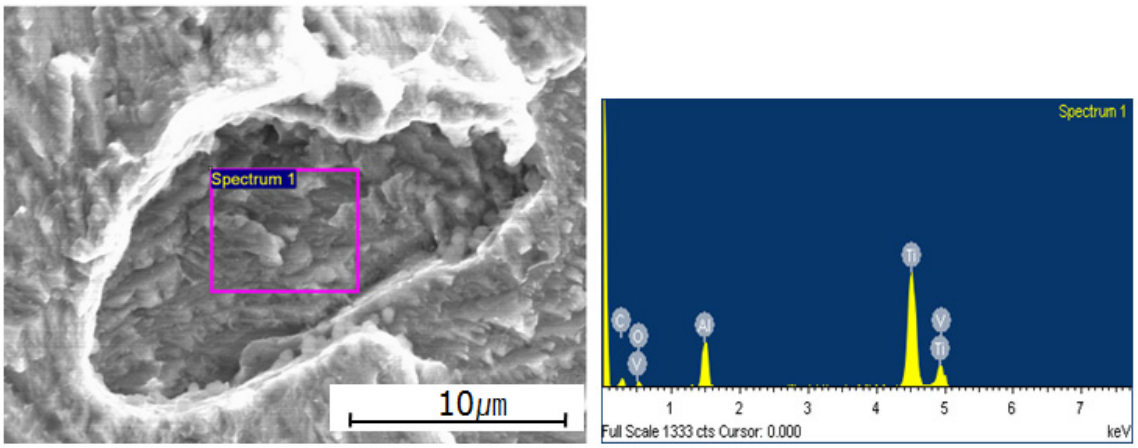

Figure 13. Energy dispersive spectroscopy (EDS) test results and SEM image of pores.

Table 5. Results of EDS test of porosity.

Identification	Weight (%)
C	7.33
O	10.77
Al	9.56
Ti	70.26
V	2.08

4. Discussion

4.1. The TIG Dressing Reheating Effects on Weld Pore Redistribution

The driving forces for fluid flow in the weld pool include the buoyancy force, the Lorentz force, the surface tension force, and the arc shear stress. In the case of the TIG welding, especially below 200 A welding parameters, the effect of arc shear stress on fluid flow is small, and the maximum velocity of buoyancy convection is far less than the forced convection driven by the Lorentz force. Therefore, the effects of arc shear stress and the buoyancy force on the pore removal mechanism by the TIG dressing can be ignored [23].

In this study, the TIG dressing was applied to a back bead region, which is different from a welded surface. As a result, weld pores that formed along the fusion line and the edge region of the weldment moved along the fluid flow of the molten pool, which moves from the center of the weldment to the

edge because of the Lorentz force, as shown in Figure 14. Because of this reason, it was to be considered that the pores located near the surface area were to be removed. It was not able to verify the effect of the TIG dressing on pores size greater than 300 μm. Such a verification would require in-depth research on whether fluid flow due to the Lorentz force can influence the movement of pores greater than a certain size and whether energy exceeding the surface tension of the weld pool can be acquired when pores greater than a certain size are removed.

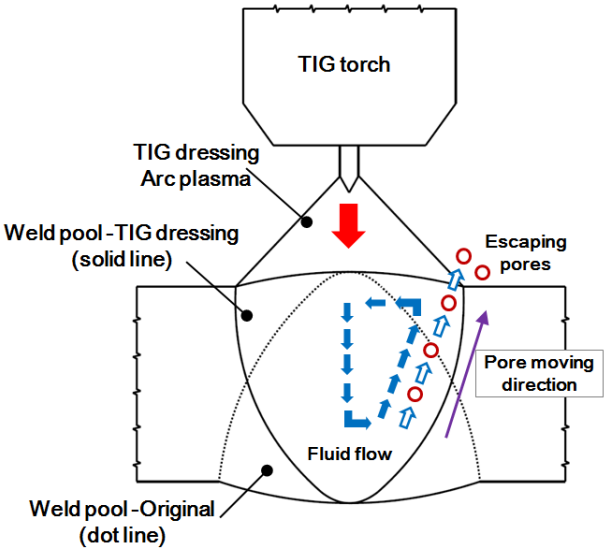

Figure 14. Schematic diagram of porosity escape.

4.2. Porosity Nucleation and Crack Mechanism

It is believed that bubble nucleation in a weld pool is heterogeneous nucleation that occurs at the boundary between the solid state and liquid state when dissolved gas exceeds its solubility. When a molten weld pool passes along the weld seam, dissolved gases from absorbed gas-forming substances act as nucleation sites for gas bubbles. The higher amount of oxygen in the pores is evidence of this mechanism. Previous studies have suggested that local embrittlement around the pores caused pore cracking. However, these previous studies did not identify any microstructural or hardness changes that could be associated with or attributed to the presence of pores. It has been suggested that embrittlement may be caused by gases present within the pores. Interstitial elements, such as oxygen, may cause local embrittlement. However, there is no metallurgical or experimental evidence of this local embrittlement around pores.

Pores that form in a titanium alloy weldment are formed at the edge of the weldment. In the weldment, the LBZ (local brittle zone) is formed along the fusion line where the parent material and welding consumables meet. The LBZ is highly brittle and is a starting point for weld fracture. In a titanium alloy weldment, weld pores form around the LBZ. Weld cracks are generated around the pores in titanium alloy weldments by complex processes that result from residual stress after welding, as pores are formed in the LBZ, which has relatively low toughness (high hardness) in comparison to the surrounding region as shown in Figure 15. The explanation for the initiation of fracture from the lowest-toughness region via the formation of a crack tip under loading is known as fracture theory. Pores are believed to act as crack tips for fracture initiation in the local brittle zone, and stress concentration due to pores geometrical effects under loading is believed to be the driving force of crack propagation.

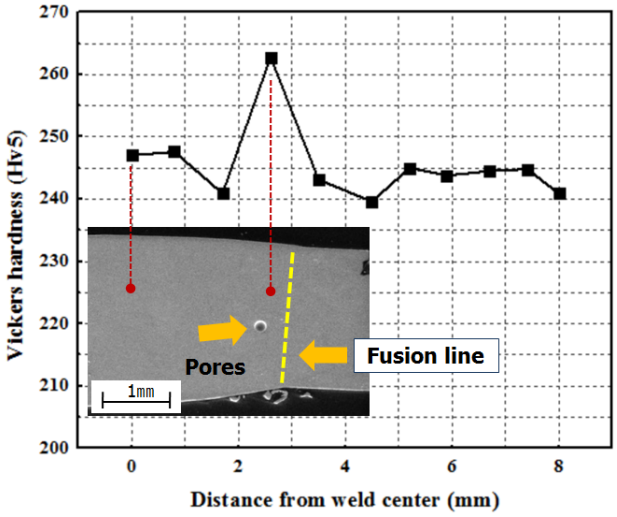

Figure 15. Hardness distribution of titanium weldment (WO).

5. Conclusions

In this study, Weld porosity redistribution due to TIG dressing and the effects of TIG dressing on the mechanical properties of titanium alloy weldments were analyzed. Additionally, the weld porosity in Ti-3Al-2.5V pipe weldments and the phenomenon of cracks due to weld porosity were observed and studied. Our findings are as follows:

1 Weld pores less than 300 μm in size were redistributed or removed via TIG dressing remelting.
2 Regardless of the tensile test temperature, the NSR rate recorded was greater than 1.0. There was a loss of 7% in the ambient- and high-temperature tensile strength of the weldments after one, two, and three TIG dressing applications, compared with the original weldment.
3 Examination of weldments in which cracking occurred showed that weld porosity was generated along the crack propagation path, that cracks were propagated through intragranular fracture, and that branch cracks were created.
4 With respect to the pore cracking mechanism, it is suggested that local features (pores forming in local brittle zones) and geometric features (stress concentration) of the pore have significant effects on crack initiation and propagation under loading conditions.

Author Contributions: Hui-Jun Yi conceived, designed and performed the experiments and wrote the papers. Yong-Jun Lee and Kwang-O Lee contributed analysis tools and reviewed papers.

Conflicts of Interest: The authors declare no conflict of interest.

References

1. Christoph, L.; Manfred, P. *Titanium and Titanium Alloys-Fundamentals and Application*, 1st ed.; Wiley-VCH: Weinheim, Germany, 2003.
2. Lutjering, G.; Williams, J.C. *Titanium*, 1st ed.; Springer: New York, NY, USA, 2007.
3. Donachie, M.J. *Titanium and Titanium Alloys*, 1st ed.; American Society for Matals: Material Park, OH, USA, 1982.
4. Williams, J.C.; Edgar, A.; Starke, J. Progress in structural materials for aerospace systems. *Acta Mater.* **2003**, *51*, 5775–5799. [CrossRef]
5. Huang, J.L.; Warnken, N.; Gebelin, J.C.; Stangwood, M.; Reed, R.C. On the mechanism of porosity formation during welding of titanium. *Acta Mater.* **2012**, *60*, 3215–3225. [CrossRef]
6. Boyer, R.R. Use of titanium in the aerospace industry. *Mater. Sci. Eng. A* **1996**, *213*, 103–114. [CrossRef]
7. Gouret, N.; Dour, G.; Miguet, B.; Oliver, E.; Fortunier, R. Assessment of the origin of porosity in electron-beam-welded TA6V plates. *Metall. Mater. Trans. A* **2004**, *35*, 879–889. [CrossRef]

8. Lee, P.D.; Hunt, J.D. Hydrogen porosity in directional solidified aluminium-copper alloys: In situ observation. *Acta Mater.* **1997**, *45*, 4155–4169. [CrossRef]
9. Atwood, R.C.; Sridhar, S.; Zhang, W.; Lee, P.D. Diffusion-controlled growth of hydrogen pores in aluminium-sillcon casting: In situ obervation and modelling. *Acta Mater.* **2000**, *48*, 405–417. [CrossRef]
10. Kornilov, I.I.; Baikow, A.A. Effect of oxygen on titnaium and its alloys. *Inst. Metall.* **1973**, *10*, 2–6.
11. Matyushkin, B.A.; Gorshkov, A.I.; Murav'ev, V.I. Special features of formation and development of cracks and pores in the metal of welds of titanium alloys after the welding. *Svarochn. Proizv.* **1975**, *8*, 9–11.
12. Smith, L.S.; Gittos, M.F. *Hydride Cracking in Titanium and Its Alloys*; TWI Reasrch Report 658/1998; TWI: Cambridge, UK, 1998.
13. Bettles, C.J.; Tomus, D.D.; Gibson, M.A. The role of microsturcture in the mechanical behavior of Ti-1.6 wt % Fe alloys contaning O and N. *Mater. Sci. Eng. A* **2011**, *528*, 4899–4909. [CrossRef]
14. Fuji, A.; Horiuchi, Y.; Yamamoto, K. Friction welidng of pure titanium and pure nickel. *Sci. Tech. Weld. Join.* **2005**, *10*, 287–294. [CrossRef]
15. Atwood, R.C.; Lee, P.D. Simulation of the three-dimessional morphology of solidification porosity in an aluminium-silicon alloy. *Acta Mater.* **2003**, *51*, 5447–5466. [CrossRef]
16. Khaled, T. An inverstigation of pore cracking in titanium welds. *J. Mater. Eng. Perform.* **1992**, *3*, 419–434. [CrossRef]
17. Wu, H.; Feng, J.; He, J. Microstructure evolution and fracture behaviour for electron beam welding of Ti-6Al-4V. *Bull. Mater. Sci.* **2004**, *27*, 387–392. [CrossRef]
18. Liu, J.; Dahmen, M.; Ventzke, V.; Kashaev, N.; Poprawe, R. The effect of heat treatment on crack control and grain refinement in laser beam welded β-solidifying TiAl-based alloy. *Intermetallics* **2013**, *40*, 65–70. [CrossRef]
19. Kim, Y.W.; Kim, S.L. Effects of microstructure and C and Si additions on elevated temperature creep and fatigue of gamma TiAl alloys. *Intermetallics* **2014**, *53*, 92–101. [CrossRef]
20. Haagensen, P.J.; Maddox, S.J. *IIW Recommendations on Post Weld Improvement of Steel and Aluminum Structures*; The International Institute of Welding: Roissy, France, 2008; XIII-2200r1-07.
21. Kado, S. Influence of the Conditions in TIG Dressing on the Fatigue Strength in Welded High Tensile Strength Steels. The International Institute of Welding: Roissy, France, 1975; XIII-771-75.
22. Redchits, V. Scientific fundamentals and measures used to prevent the formation of pores in fusion welded titanium and its alloys. *Weld. Int.* **1997**, *11*, 722–728. [CrossRef]
23. Kou, S. *Welding Metallurgy*, 2nd ed.; John Wiley and Sons: New York, NY, USA, 2001.

© 2016 by the authors; licensee MDPI, Basel, Switzerland. This article is an open access article distributed under the terms and conditions of the Creative Commons Attribution (CC-BY) license (http://creativecommons.org/licenses/by/4.0/).